

Tri-resonant leptogenesis from modular symmetry neutrino models

Zhen-hua Zhao¹, Zhi-Cheng Liu^{2*}

¹ Department of Physics, Liaoning Normal University, Dalian 116029, China

² School of Materials Science and Engineering, Anyang Institute of Technology,
Anyang 455000, China

Abstract

In this paper, we have studied the consequences of some representative modular symmetry neutrino models for tri-resonant leptogenesis (which is realized by having three nearly degenerate right-handed neutrinos). To be specific, we have considered modular A_4 , S_4 and A_5 symmetry models that have a right-handed neutrino mass matrix M_R as shown in Eq. (5) which gives three degenerate right-handed neutrino masses and consequently prohibits the leptogenesis mechanism to work. For these models, we have considered two minimal ways to generate the desired small mass splittings among the three right-handed neutrinos: one scenario is to modify M_R to a form as shown in Eq. (7), while another scenario is to consider the renormalization-group corrections for the right-handed neutrino masses. In the former scenario, for the considered models, the observed value of η_B can always be successfully reproduced for appropriate values of μ . But in the latter scenario not all the considered models can successfully reproduce the observed value of η_B .

arXiv:2405.09363v1 [hep-ph] 15 May 2024

*Corresponding author: liuzhicheng230911@126.com

1 Introduction

As we know, the discovery of neutrino oscillations reveals that neutrinos are massive and their flavor eigenstates ν_α (for $\alpha = e, \mu, \tau$) are certain superpositions of their mass eigenstates ν_i (for $i = 1, 2, 3$) possessing definite masses m_i : $\nu_\alpha = \sum_i U_{\alpha i} \nu_i$ with $U_{\alpha i}$ being the αi -th element of the neutrino mixing matrix U [1]. In the standard form, U is expressed in terms of three mixing angles θ_{ij} (for $ij = 12, 13, 23$), one Dirac CP phase δ and two Majorana CP phases α_{21} and α_{31} as

$$U = \begin{pmatrix} c_{12}c_{13} & s_{12}c_{13} & s_{13}e^{-i\delta} \\ -s_{12}c_{23} - c_{12}s_{23}s_{13}e^{i\delta} & c_{12}c_{23} - s_{12}s_{23}s_{13}e^{i\delta} & s_{23}c_{13} \\ s_{12}s_{23} - c_{12}c_{23}s_{13}e^{i\delta} & -c_{12}s_{23} - s_{12}c_{23}s_{13}e^{i\delta} & c_{23}c_{13} \end{pmatrix} \begin{pmatrix} 1 & & \\ & e^{i\alpha_{21}} & \\ & & e^{i\alpha_{31}} \end{pmatrix}, \quad (1)$$

where the abbreviations $c_{ij} = \cos \theta_{ij}$ and $s_{ij} = \sin \theta_{ij}$ have been employed.

Nowadays, the neutrino mixing angles and neutrino mass squared differences $\Delta m_{ij}^2 \equiv m_i^2 - m_j^2$ have been measured to good degrees of accuracy, and there is also a preliminary result for δ (but with a large uncertainty). Several research groups have performed global analyses of the existing neutrino oscillation data to extract the values of these parameters [2, 3]. For reference, the results in Ref. [2] are reproduced in Table 1 here. Note that the sign of Δm_{31}^2 remains undetermined, thereby allowing for two possible neutrino mass orderings: the normal ordering (NO) $m_1 < m_2 < m_3$ and inverted ordering (IO) $m_3 < m_1 < m_2$. However, neutrino oscillations are completely insensitive to the absolute neutrino mass scale and the Majorana CP phases. Their values can only be inferred from certain non-oscillatory experiments such as the neutrinoless double beta decay experiments [4]. But so far there has not been any lower bound on the lightest neutrino mass, nor any constraint on the Majorana CP phases.

For the neutrino mixing angles, Table 1 shows that θ_{12} and θ_{23} are close to some special values (i.e., $\sin^2 \theta_{12} \sim 1/3$ and $\sin^2 \theta_{23} \sim 1/2$). But θ_{13} is relatively small. In fact, before its value was measured, θ_{13} had been widely expected to be vanishingly small. For the ideal case of $\sin^2 \theta_{12} = 1/3$, $\sin^2 \theta_{23} = 1/2$ and $\theta_{13} = 0$, the neutrino mixing matrix takes a very simple form as

$$U_{\text{TBM}} = \frac{1}{\sqrt{6}} \begin{pmatrix} 2 & \sqrt{2} & 0 \\ 1 & -\sqrt{2} & -\sqrt{3} \\ 1 & -\sqrt{2} & \sqrt{3} \end{pmatrix}, \quad (2)$$

which is referred to as the tribimaximal (TBM) mixing [5]. This particular mixing has inspired intensive model-building studies with the employment of certain discrete non-Abelian symmetries (e.g., A_4 and S_4) [6].

Noteworthy, a shortcoming of the conventional flavor-symmetry models is that many flavon fields need to be introduced in order to achieve a desired breaking pattern of the flavor symmetry, and the scalar potential of these flavon fields needs a complicated symmetric shaping. Moreover, higher-dimensional operators with more flavon insertions and unknown coefficients are often present, affecting the predictive power of the models. In recent years, the idea of modular invariance which provides substantial simplifications to these problems has been proposed and become increasingly popular [7, 8]. In the modular-invariance approach, the flavour symmetry is broken by the VEV of a single scalar field—the so-called modulus, while the flavon fields are not necessary. And the Yukawa couplings and fermion mass

	Normal Ordering		Inverted Ordering	
	bf μ $\pm 1\sigma$	3σ range	bf μ $\pm 1\sigma$	3σ range
$\sin^2 \theta_{12}$	$0.303^{+0.012}_{-0.011}$	$0.270 \rightarrow 0.341$	$0.303^{+0.012}_{-0.011}$	$0.270 \rightarrow 0.341$
$\sin^2 \theta_{23}$	$0.572^{+0.018}_{-0.023}$	$0.406 \rightarrow 0.620$	$0.578^{+0.016}_{-0.021}$	$0.412 \rightarrow 0.623$
$\sin^2 \theta_{13}$	$0.02203^{+0.00056}_{-0.00059}$	$0.02029 \rightarrow 0.02391$	$0.02219^{+0.00060}_{-0.00057}$	$0.02047 \rightarrow 0.02396$
δ/π	$1.09^{+0.23}_{-0.14}$	$0.96 \rightarrow 1.33$	$1.59^{+0.15}_{-0.18}$	$1.41 \rightarrow 1.74$
$\Delta m_{21}^2/(10^{-5} \text{ eV}^2)$	$7.41^{+0.21}_{-0.20}$	$6.82 \rightarrow 8.03$	$7.41^{+0.21}_{-0.20}$	$6.82 \rightarrow 8.03$
$\Delta m_{3\ell}^2/(10^{-3} \text{ eV}^2)$	$2.511^{+0.028}_{-0.027}$	$2.428 \rightarrow 2.597$	$-2.498^{+0.032}_{-0.025}$	$-2.581 \rightarrow -2.408$

Table 1: The best-fit values, 1σ errors and 3σ ranges of six neutrino oscillation parameters extracted from a global analysis of the existing neutrino oscillation data as of November 2022 [2], where $m_{3\ell}^2 = m_{31}^2 > 0$ for NO and $m_{3\ell}^2 = m_{32}^2 > 0$ for IO .

terms are certain special functions of the modulus called modular forms that have particular properties under the modular group transformations. Moreover, all higher-dimensional operators are unambiguously determined in the limit of unbroken supersymmetry. As a result, flavor models with modular invariance depend on fewer parameters, enhancing their predictive power.

As for the neutrino masses, one of the most popular and natural ways of generating them is the type-I seesaw model [9] in which three heavy right-handed neutrinos N_I ($I = 1, 2, 3$) are introduced into the Standard Model (SM). First of all, N_I can constitute the Yukawa coupling operators together with the lepton doublets L_α and the Higgs doublet H : $Y_{I\alpha} \overline{N}_I H L_\alpha$ with $Y_{I\alpha}$ being the $I\alpha$ -th element of the Yukawa coupling matrix Y . These operators will generate the Dirac neutrino mass terms $(M_D)_{I\alpha} = Y_{I\alpha} v$ [here $(M_D)_{I\alpha}$ is the $I\alpha$ -th element of the Dirac neutrino mass matrix M_D] after the neutral component of H acquires a nonzero vacuum expectation value (VEV) $v = 174 \text{ GeV}$. In addition, N_I themselves can also have the Majorana mass terms $\overline{N}_I (M_R)_{IJ} N_J^c$ [here $(M_R)_{IJ}$ are the IJ -th element of the right-handed neutrino mass matrix M_R]. Then, under the seesaw condition $M_R \gg M_D$, integrating the right-handed neutrinos out yields an effective Majorana mass matrix for three light neutrinos as

$$M_\nu = -M_D^T M_R^{-1} M_D . \quad (3)$$

Here we would like to point out that throughout the paper the fermion mass matrices are written in the right-left convention which is more conveniently used in the supersymmetric setup as applicable to our study.

Remarkably, the seesaw model also provides an attractive explanation (which is known as the leptogenesis mechanism [10, 11]) for the baryon-antibaryon asymmetry of the Universe [12]

$$Y_B \equiv \frac{n_B - n_{\overline{B}}}{s} \simeq (8.69 \pm 0.04) \times 10^{-11} , \quad (4)$$

where n_B ($n_{\overline{B}}$) denotes the baryon (antibaryon) number density and s the entropy density. The leptogenesis mechanism works in a way as follows: a lepton-antilepton asymmetry $Y_L \equiv (n_L - n_{\overline{L}})/s$ is firstly generated from the out-of-equilibrium and CP-violating decays of the right-handed neutrinos and then partly converted into the baryon-antibaryon asymmetry via the sphaleron processes: $Y_B \simeq -cY_L$ with

$c = 28/79$ or $8/23$ in the SM or MSSM (Minimal Supersymmetric Standard Model) framework. As is known, in the scenario that the right-handed neutrino masses are hierarchical there exists a lower bound about 10^9 GeV for the right-handed neutrino mass scale in order to successfully reproduce the observed value of Y_B [13]. Obviously, such a high right-handed neutrino mass scale has no chance to be directly accessed by foreseeable collider experiments. Fortunately, in the resonant leptogenesis scenario which is realized for nearly degenerate right-handed neutrinos [14], a successful leptogenesis can be realized even with TeV-scale right-handed neutrinos which have the potential to be directly accessed by running or upcoming experiments [15].

However, for some typical modular symmetry neutrino models (see the models provided in sections 3-5), the right-handed neutrino mass matrix takes a form as

$$M_R = \begin{pmatrix} M_0 & 0 & 0 \\ 0 & 0 & M_0 \\ 0 & M_0 & 0 \end{pmatrix}. \quad (5)$$

It can be diagonalized by the following unitary matrix

$$U_R = \begin{pmatrix} 0 & 1 & 0 \\ \frac{i}{\sqrt{2}} & 0 & \frac{1}{\sqrt{2}} \\ -\frac{i}{\sqrt{2}} & 0 & \frac{1}{\sqrt{2}} \end{pmatrix}, \quad (6)$$

to give three degenerate right-handed neutrino masses (i.e., M_0). In this case, unfortunately, the leptogenesis mechanism is prohibited to work. But just as a coin has two sides, this kind of models can serve as a unique basis for realizations of the tri-resonant leptogenesis scenario: if the right-handed neutrino masses receive certain corrections so that their degeneracy is lifted to an appropriate extent, then the tri-resonant leptogenesis scenario will be naturally realized [†].

In this paper, we consider two minimal ways to generate the desired small mass splittings among the three right-handed neutrinos: one way is to modify M_R to a form as

$$M_R = \begin{pmatrix} M_0 & 0 & 0 \\ 0 & \mu & M_0 \\ 0 & M_0 & \mu \end{pmatrix}. \quad (7)$$

with $\mu \ll M_0$. Such a modification of M_R has the merit that it only introduces one additional parameter and it still can be diagonalized by the unitary matrix U_R in Eq. (6) (i.e., it does not alter the original neutrino mixing pattern). But the three right-handed neutrino masses are modified to $M_0 - \mu$, M_0 and $M_0 + \mu$, respectively. Another way is to consider the renormalization-group corrections for the right-handed neutrino masses [17]: if the energy scale Λ_{FS} of the flavor-symmetry physics that shapes the special textures of neutrino mass matrices is much higher than the right-handed neutrino mass scale M_0 where leptogenesis takes place (such a scenario is very likely given that the idea of modular flavor symmetry is just inspired from the string theory [7]), then the renormalization group evolution (RGE) effect between the scales of Λ_{FS} and M_0 may induce some mass splittings among the three right-handed

[†]For a realization of resonant leptogenesis in the minimal seesaw model with a modular symmetry, see Ref. [16].

neutrinos (see section 2.2). Such a correction of M_R has the following two merits: 1) this effect is spontaneous, provided that there is a considerable gap between the flavor-symmetry scale and the right-handed neutrino mass scale; 2) this effect is minimal, in the sense that it does not need to introduce additional parameters.

The remaining parts of this paper are organized as follows. In section 2 we will first give some basic formulas about resonant leptogenesis and RGE effects that will be used in our study. Then, we perform the study for three representative modular symmetry models which contain three degenerate right-handed neutrinos. We first consider the modular A_4 symmetry model in section 3, then the modular S_4 symmetry model in section 4, and finally the modular A_5 symmetry model in section 5. In section 6, we summarize our main results.

2 Resonant leptogenesis and RGE effects

2.1 Some basics about resonant leptogenesis

As is known, if the temperature T of the Universe at which leptogenesis takes place (approximately the right-handed neutrino mass scale) is below 10^9 GeV, all the three lepton flavors have become distinguishable from one another and the lepton asymmetries stored in them should be tracked separately [18]. Such a three-flavor regime applies to the scenario studied in this paper (i.e., low-scale tri-resonant leptogenesis). In this case, the final lepton asymmetry can be approximately expressed as

$$Y_L \simeq r(\varepsilon_e \kappa_e + \varepsilon_\mu \kappa_\mu + \varepsilon_\tau \kappa_\tau). \quad (8)$$

Here the factor $r \simeq 4 \times 10^{-3}$ measures the ratio of the equilibrium number density of right-handed neutrinos to the entropy density. And ε_e is a sum over three right-handed neutrinos (i.e., $\varepsilon_e = \varepsilon_{1e} + \varepsilon_{2e} + \varepsilon_{3e}$) of the following CP asymmetries:

$$\varepsilon_{I\alpha} \equiv \frac{\Gamma(N_I \rightarrow L_\alpha + H) - \Gamma(N_I \rightarrow \bar{L}_\alpha + \bar{H})}{\sum_\alpha \Gamma(N_I \rightarrow L_\alpha + H) + \Gamma(N_I \rightarrow \bar{L}_\alpha + \bar{H})}, \quad (9)$$

whose explicit expressions will be given below. Finally, κ_α are the efficiency factors (which are smaller than 1) due to the washout effects. Their concrete values can be calculated by numerically solving relevant Boltzmann equations, whose explicit expressions will also be given below.

To be explicit, in the basis where both the right-handed neutrino matrix and charged lepton mass matrix are diagonal, the CP asymmetries $\varepsilon_{I\alpha}$ defined in Eq. (9) can be expressed as [14]

$$\varepsilon_{I\alpha} = \frac{|\bar{Y}_+{}_{I\alpha}|^2 - |\bar{Y}_-{}_{I\alpha}|^2}{\left(\bar{Y}_+ \bar{Y}_+^\dagger\right)_{II} + \left(\bar{Y}_- \bar{Y}_-^\dagger\right)_{II}}. \quad (10)$$

Here $(\bar{Y}_\pm)_{I\alpha}$ are the effective neutrino Yukawa couplings in the case of there existing three nearly degenerate right-handed neutrinos. They can be expressed as

$$\begin{aligned} (\bar{Y}_\pm)_{I\alpha} = & Y_{I\alpha} - iV_{I\alpha} + i \sum_{J,K=1}^3 |\epsilon_{IJK}| Y_{J\alpha} \\ & \times \frac{M_I (\mathcal{M}_{IIJ} + \mathcal{M}_{JJI}) + iR_{IK} [\mathcal{M}_{IKJ} (\mathcal{M}_{IIK} + \mathcal{M}_{KKI}) + \mathcal{M}_{JJK} (\mathcal{M}_{IKI} + \mathcal{M}_{KIK})]}{M_I^2 - M_J^2 - 2iM_I^2 A_{JJ} - 2i\text{Im}(R_{IK}) [M_I^2 |A_{JK}|^2 + M_J M_K \text{Re}(A_{JK}^2)]}, \end{aligned} \quad (11)$$

where ϵ_{IJK} is the anti-symmetric Levi-Civita symbol, $\mathcal{M}_{IJK} \equiv M_I A_{JK}$ and

$$A_{IJ} = \frac{(YY^\dagger)_{IJ}^*}{16\pi}, \quad V_{I\alpha} = \sum_{\beta=e,\mu,\tau} \sum_{K \neq I} \frac{Y_{I\beta}^* Y_{K\beta} Y_{K\alpha}}{16\pi} f\left(\frac{M_K^2}{M_I^2}\right),$$

$$R_{IJ} = \frac{M_I^2}{M_I^2 - M_J^2 - 2iM_I^2 A_{JJ}}, \quad (12)$$

with $f(x) = \sqrt{x}[1 - (1+x)\ln(1+1/x)]$ being the loop function. And the corresponding CP-conjugate effective Yukawa couplings $(\bar{Y}_-)_{I\alpha}$ can be obtained by simply making the replacement $Y_{I\alpha} \rightarrow Y_{I\alpha}^*$ in the above expressions. Furthermore, in terms of these effective Yukawa couplings, the decay widths of right-handed neutrinos can be expressed as

$$\Gamma(N_I \rightarrow L_\alpha + H) = \frac{M_I}{16\pi} |(\bar{Y}_+)_{I\alpha}|^2, \quad \Gamma(N_I \rightarrow \bar{L}_\alpha + \bar{H}) = \frac{M_I}{16\pi} |(\bar{Y}_-)_{I\alpha}|^2, \quad (13)$$

and their branching ratios are given by

$$B_{I\alpha} = \frac{|(\bar{Y}_+)_{I\alpha}|^2 + |(\bar{Y}_-)_{I\alpha}|^2}{(\bar{Y}_+ \bar{Y}_+^\dagger)_{II} + (\bar{Y}_- \bar{Y}_-^\dagger)_{II}}. \quad (14)$$

In order to generate a nonzero lepton asymmetry in the Universe, one needs not only the above CP asymmetries, but also a departure from thermal equilibrium. In the latter processes, the evolutions of the number densities of the right-handed neutrinos n_{N_I} and flavored lepton asymmetries n_{L_α} (which are normalized by the photon number density n_γ to $\eta_{N_I} \equiv n_{N_I}/n_\gamma$ and $\eta_{L_\alpha} \equiv n_{L_\alpha}/n_\gamma$, respectively) can be tracked by the following Boltzmann equations [14]

$$\begin{aligned} \frac{d\eta_{N_I}}{dz} &= \frac{z}{H(z=1)} \left[\left(1 - \frac{\eta_{N_I}}{\eta_{N_I}^{\text{eq}}}\right) \sum_{\alpha=e,\mu,\tau} \left(\Gamma^{D(I\alpha)} + \Gamma_{\text{Yukawa}}^{S(I\alpha)} + \Gamma_{\text{Gauge}}^{S(I\alpha)} \right) \right. \\ &\quad \left. - \frac{2}{3} \sum_{\alpha=e,\mu,\tau} \eta_{L_\alpha} \varepsilon_{I\alpha} \left(\hat{\Gamma}^{D(I\alpha)} + \hat{\Gamma}_{\text{Yukawa}}^{S(I\alpha)} + \hat{\Gamma}_{\text{Gauge}}^{S(I\alpha)} \right) \right], \\ \frac{d\eta_{L_\alpha}}{dz} &= \frac{z}{H(z=1)} \left\{ \sum_{I=1}^3 \varepsilon_{I\alpha} \left(\frac{\eta_{N_I}}{\eta_{N_I}^{\text{eq}}} - 1 \right) \sum_{\beta=e,\mu,\tau} \left(\Gamma^{D(I\beta)} + \Gamma_{\text{Yukawa}}^{S(I\beta)} + \Gamma_{\text{Gauge}}^{S(I\beta)} \right) \right. \\ &\quad - \frac{2}{3} \eta_{L_\alpha} \left[\sum_{I=1}^3 B_{I\alpha} \left(\tilde{\Gamma}^{D(I\alpha)} + \tilde{\Gamma}_{\text{Yukawa}}^{S(I\alpha)} + \tilde{\Gamma}_{\text{Gauge}}^{S(I\alpha)} + \Gamma_{\text{Yukawa}}^W(I\alpha) + \Gamma_{\text{Gauge}}^W(I\alpha) \right) \right. \\ &\quad \left. \left. + \sum_{\beta=e,\mu,\tau} \left(\Gamma_{\text{Yukawa}}^{\Delta L=2(\alpha\beta)} + \Gamma_{\text{Yukawa}}^{\Delta L=0(\alpha\beta)} \right) \right] \right. \\ &\quad \left. - \frac{2}{3} \sum_{\beta=e,\mu,\tau} \eta_{L_\beta} \left[\sum_{I=1}^3 \varepsilon_{I\alpha} \varepsilon_{I\beta} \left(\Gamma_{\text{Yukawa}}^W(I\beta) + \Gamma_{\text{Gauge}}^W(I\beta) + \Gamma_{\text{Yukawa}}^{\Delta L=2(\alpha\beta)} - \Gamma_{\text{Yukawa}}^{\Delta L=0(\alpha\beta)} \right) \right] \right\}, \quad (15) \end{aligned}$$

where $z = M_1/T$ has been defined, and

$$H(z) = \sqrt{\frac{4\pi^3 g_*}{45}} \frac{M_1^2}{z^2 M_{\text{Pl}}}, \quad (16)$$

is the Hubble parameter with $M_{\text{Pl}} = 1.221 \times 10^{19} \text{ GeV}$ and $g_* \simeq 106.75$ or 228.75 (in the SM and MSSM frameworks, respectively) being the number of relativistic degrees of freedom in the early Universe. And the analytical expressions of the Γ terms on the right-hand side of Eq. (15) can be found in Ref. [14]. Note that at the present epoch one has the relation $s \simeq 7.04 n_\gamma$ for the entropy and photon number densities, and correspondingly $Y_L \simeq \eta_L/7.04$ (with $\eta_L = \eta_{L_e} + \eta_{L_\mu} + \eta_{L_\tau}$).

2.2 Some basics about RGE effects

As mentioned in the introduction section, the flavor-symmetry models which contain three degenerate right-handed neutrinos serve as a unique basis for realizations of the tri-resonant leptogenesis scenario after the right-handed neutrino masses receive certain corrections so that their degeneracy is lifted to an appropriate extent. And the renormalization group evolution effects from high to low energies can play the role of generating the desired right-handed neutrino mass splittings. In the literature, most of the flavor-symmetry models have been formulated in the MSSM framework for the following reason: in order to break the flavor symmetry in a proper way, one needs to introduce some flavon fields which transform as multiplets of the flavor symmetry and develop particular VEV alignments; and the most popular and perhaps natural approach to derive the desired flavon VEV alignments is provided by the so-called F-term alignment mechanism which is realized in a supersymmetric setup [6]. In particular, all of the modular flavor-symmetry models have been formulated in the MSSM framework since the modular flavor symmetry needs supersymmetry to preserve the holomorphicity of the modular form [7]. For these reasons, we will perform our study in the MSSM framework.

In the MSSM framework, the one-loop RGE evolution of the right-handed neutrino mass matrix and the Dirac neutrino Yukawa matrix Y in the basis where M_R is diagonal are given by [19]

$$\begin{aligned} 4\pi^2 \frac{dM_I}{dt} &= (YY^\dagger)_{II} M_I, \\ 16\pi^2 \frac{dY}{dt} &= -T^*Y - Y \left[\alpha - (3Y^\dagger Y + Y_l^\dagger Y_l) \right], \end{aligned} \quad (17)$$

where $t = \ln(M_0/\mu)$ has been defined, with M_0 and μ denoting the right-handed neutrino mass scale and renormalization scale, respectively. $\alpha = 3g_2^2 + \frac{3}{5}g_1^2 - \text{Tr}(3Y_U^\dagger Y_U + Y^\dagger Y)$, g_2 and g_1 are the $SU(2)_L$ and $U(1)_Y$ gauge coupling constants, and $Y_{U,l}$ are the Yukawa matrices for up-type quarks and charged leptons. T is a 3×3 anti-Hermitian matrix and its entries are given by

$$\begin{aligned} T_{II} &= 0, \\ T_{IJ} &= -T_{JI}^* = \frac{M_J + M_I}{M_J - M_I} \text{Re}[(YY^\dagger)_{IJ}] + i \frac{M_J - M_I}{M_J + M_I} \text{Im}[(YY^\dagger)_{IJ}], \quad \text{for } I \neq J. \end{aligned} \quad (18)$$

T_{IJ} is singular at the scale where $M_J = M_I$ holds unless $\text{Re}[(YY^\dagger)_{IJ}] = 0$. To achieve this condition, we perform an additional rotation in the above basis:

$$M'_R = O^\dagger M_R O^* = M_R, \quad Y' = O^\dagger Y, \quad (19)$$

where O is a real orthogonal matrix which can be parameterized by three angles $\theta_{1,2,3}$. This rotation does not affect the right-handed neutrino mass matrix due to their exact mass degeneracy. YY^\dagger becomes

$$Y'Y'^\dagger = O^\dagger YY^\dagger O. \quad (20)$$

Apparently, the three condition $\text{Re}[(YY^\dagger)_{IJ}] = 0$ can be always satisfied by choosing suitable values of $\theta_{1,2,3}$. The RGE evolution of the right-handed neutrino mass matrix in the new basis is

$$4\pi^2 \frac{dM_I}{dt} = (Y'Y'^\dagger)_{II} M_I. \quad (21)$$

For illustration, taking account of the RGE effects from the flavor-symmetry scale Λ_{FS} to the right-handed neutrino mass scale M_0 , one can obtain the following relation for the right-handed neutrino masses

$$M_I(M_0) \simeq M_I(\Lambda_{\text{FS}}) \left[1 - \frac{1}{4\pi^2} \left(Y'Y'^{\dagger} \right)_{II} \ln \left(\frac{\Lambda_{\text{FS}}}{M_0} \right) \right], \quad (22)$$

yielding the following mass splittings for the right-handed neutrinos

$$M_I(M_0) - M_J(M_0) \simeq \frac{M_I(\Lambda_{\text{FS}})}{4\pi^2} \left[\left(Y'Y'^{\dagger} \right)_{JJ} - \left(Y'Y'^{\dagger} \right)_{II} \right] \ln \left(\frac{\Lambda_{\text{FS}}}{M_0} \right). \quad (23)$$

Such mass splittings among the right-handed neutrinos are comparable to their decay widths

$$\Gamma_I = \frac{(YY^{\dagger})_{II}}{8\pi} M_I(M_0), \quad (24)$$

fulfilling the condition for the resonant leptogenesis to proceed. Note that in obtaining Eq. (22), as a rough estimate, we have only considered the diagonal-term [i.e., $(YY^{\dagger})_{II}$ -related] contributions to the right-handed neutrino masses. But the off-diagonal-term [i.e., $(YY^{\dagger})_{IJ}$ -related] contributions may be equally important in the case of the right-handed neutrino masses being degenerate, so in the following calculations we will also consider them.

3 Study for modular A_4 symmetry model

In Ref. [20], the authors have presented a comprehensive analysis of neutrino masses and mixing in theories with modular A_4 symmetry. A_4 is the symmetry group of the even permutations of 4 objects, and it has three singlet representations $\mathbf{1}$, $\mathbf{1}'$, $\mathbf{1}''$ and one three-dimensional representation $\mathbf{3}$. Note that A_4 is the smallest non-Abelian finite group which admits a three-dimensional representation (a desired feature for describing the flavor mixing of three generation fermions). In this model, both the three left-handed lepton doublets and three right handed neutrinos constitute the $\mathbf{3}$ representation of A_4 . In the case that the weights of the lepton doublets and right-handed neutrinos are $(k_L, k_{Nc}) = (2, 0)$, the modular invariance constrains the Dirac neutrino mass matrix to the following form

$$M_D = v_u \begin{pmatrix} 2g_1 Y_1 & (-g_1 + g_2) Y_3 & (-g_1 - g_2) Y_2 \\ (-g_1 - g_2) Y_3 & 2g_1 Y_2 & (-g_1 + g_2) Y_1 \\ (-g_1 + g_2) Y_2 & (-g_1 - g_2) Y_1 & 2g_1 Y_3 \end{pmatrix}, \quad (25)$$

while the right-handed neutrino mass matrix takes the same form as in Eq. (5). On the other hand, in the case that three right-handed charged leptons are successively assigned to the singlet representations $\mathbf{1}$, $\mathbf{1}''$ and $\mathbf{1}'$ of A_4 , the charged-lepton mass matrix takes a form as

$$M_l = v_d \begin{pmatrix} \alpha Y_1 & \alpha Y_3 & \alpha Y_2 \\ \beta Y_2 & \beta Y_1 & \beta Y_3 \\ \gamma Y_3 & \gamma Y_2 & \gamma Y_1 \end{pmatrix}. \quad (26)$$

In the above two equations, v_u and v_d are respectively the VEVs of the up-type and down-type Higgs fields, g_1 , g_2 , α , β and γ are simply dimensionless parameters, while Y_i are modular forms of level 3 and they can be expressed in terms of the Dedekind eta-function

$$\eta(\tau) \equiv q^{1/24} \prod_{n=1}^{\infty} (1 - q^n) \quad \text{with} \quad q = e^{i2\pi\tau}, \quad (27)$$

and its derivative (with $d\eta/d\tau$ being denoted as η') as

$$Y_1(\tau) = \frac{i}{2\pi} \left[\frac{\eta'(\tau/3)}{\eta(\tau/3)} + \frac{\eta'(\tau/3 + 1/3)}{\eta(\tau/3 + 1/3)} + \frac{\eta'(\tau/3 + 2/3)}{\eta(\tau/3 + 2/3)} - \frac{27\eta'(3\tau)}{\eta(3\tau)} \right], \quad (28)$$

$$Y_2(\tau) = \frac{-i}{\pi} \left[\frac{\eta'(\tau/3)}{\eta(\tau/3)} + \omega^2 \frac{\eta'(\tau/3 + 1/3)}{\eta(\tau/3 + 1/3)} + \omega \frac{\eta'(\tau/3 + 2/3)}{\eta(\tau/3 + 2/3)} \right], \quad (29)$$

$$Y_3(\tau) = \frac{-i}{\pi} \left[\frac{\eta'(\tau/3)}{\eta(\tau/3)} + \omega \frac{\eta'(\tau/3 + 1/3)}{\eta(\tau/3 + 1/3)} + \omega^2 \frac{\eta'(\tau/3 + 2/3)}{\eta(\tau/3 + 2/3)} \right], \quad (30)$$

with $\omega = e^{i2\pi/3}$. One can see that this model totally contains 8 real parameters: $\text{Re}(\tau)$, $\text{Im}(\tau)$, β/α , γ/α , $|g_2/g_1|$, $\arg(g_2/g_1)$, αv_d and $g_1^2 v_u^2/M_0$. The three parameters αv_d , β/α and γ/α can be fixed by fitting with the values of three charged lepton masses. The remaining parameters serve to describe the three neutrino masses, three neutrino mixing angles and three CP phases present in the neutrino mixing matrix. The detailed numerical calculation shows that this model can be consistent with the neutrino oscillation experimental results in both the NO and IO cases. And the resulting predictions for the best-fit values and the allowed ranges of the input parameters and observables are collected in Table 2.

	NO		IO	
	Best-fit	Allowed regions	Best-fit	Allowed regions
$\text{Re}(\tau)$	0.0129	[0, 0.431]	0.096	[0, 0.102]
$\text{Im}(\tau)$	1.824	[0.91, 1.16] \cup [1.31, 1.86]	0.987	[0.98, 1.049] \cup [1.052, 1.109]
β/α	205.720	[192.39, 215] \cup [3054.254093.49]	79.472	[59.68, 86.37] \cup [892.67, 1446.02]
γ/α	3612.07	[192.4, 215] \cup [3066.47, 4092.98]	1232.57	[60.97, 86.34] \cup [870.16, 1443.84]
$ g_2/g_1 $	2.410	[2.398, 2.71] \cup [2.95, 3.86]	2.093	[1.038, 2.453]
$\arg(g_2/g_1)$	6.267	[0, 0.49] \cup [6.23, 2π]	4.715	[1.33, 1.83] \cup [4.29, 5]
$\alpha v_d/\text{MeV}$	0.5179	—	1.167	—
$(g_1^2 v_u^2/M_0)/\text{eV}$	0.0111	—	0.004	—
m_e/m_μ	0.0048	[0.0046, 0.0050]	0.0048	[0.0046, 0.0050]
m_μ/m_τ	0.0564	[0.0520, 0.0610]	0.0565	[0.0520, 0.0610]
$\sin^2 \theta_{12}$	0.3096	[0.2750, 0.3500]	0.3100	[0.2750, 0.3500]
$\sin^2 \theta_{13}$	0.0226	[0.02045, 0.02439]	0.02264	[0.02068, 0.02463]
$\sin^2 \theta_{23}$	0.4638	[0.4180, 0.4676]	0.584	[0.423, 0.629]
δ/π	1.486	[0.19, 0.77] \cup [1.23, 1.84]	1.458	[0.068, 1.933]
α_{21}/π	0.068	[0, 0.23] \cup [1.77, 2]	0.138	[0, 0.19] \cup [1.8, 2]
α_{31}/π	0.948	[0.683, 1.311]	0.997	[0, 2]
m_1/eV	0.0430	[0.0225, 0.0478]	0.0494	[0.0464, 0.0526]
m_2/eV	0.0439	[0.0241, 0.0485]	0.0501	[0.0472, 0.0533]
m_3/eV	0.0661	[0.0524, 0.0716]	0.0013	[0.0007, 0.0015]
χ_{\min}^2	30.72	—	10^{-7}	—

Table 2: For the modular A_4 symmetry model given in section 3, the predictions for the best-fit values and the allowed ranges of the input parameters and observables in the NO and IO cases. These results are taken from Tables 6 and 10 in Ref. [20].

We first consider the scenario that the mass splittings among the three right-handed neutrinos are realized by modifying M_R into the form as shown in Eq. (7). In order to facilitate the leptogenesis calculation, we go to the basis where both the right-handed neutrino mass matrix and charged lepton mass matrix are diagonal with the help of U_R in Eq. (6) (which serves to diagonalize the the right-handed

neutrino mass matrix) and another unitary matrix U_L which serves to diagonalize the charged lepton mass matrix. At the same time, the neutrino Yukawa coupling matrix becomes $Y' = U_R^\dagger Y U_L$ which is relevant for the leptogenesis calculations. With help of the Eq. (10) and the fitted values of the input parameters as given in Table 2, we numerically calculate the CP asymmetries in the decays of N_I as functions of $2\mu/\Gamma_I$. The results are shown in Figure 1. Since μ is a free parameter, the resonance conditions $2\mu/\Gamma_I \simeq 1$ which enhance the CP asymmetries to their maximally allowed values can always be fulfilled. This will be helpful for us to reproduce the observed value of η_B . Figure 2 has further shown the ratios of various collision terms in the Boltzmann equations to the Hubble constant as functions of $z = M_0/T$ with $M_0 = 10^3$ GeV and $\mu = 10^{-8}$ GeV as benchmark values (see below for the reason why we have taken $\mu = 10^{-8}$ GeV as a benchmark value). We see that the scattering collision term Γ_{Gauge}^S is comparable to Γ_{Yukawa}^S , and they provide the dominant sources of the scattering collision terms in the temperature range $T > M_0$. On the other hand, in the temperature range $T < M_0$, the dominant term is Γ_{Yukawa}^D that describes the decay process. Then, the numerical scan finds the values of μ that accommodate a successful leptogenesis as functions of M_0 as shown in Figure 3. Considering that people are more interested in low-scale leptogenesis (which has the potential to be directly accessed by running or upcoming experiments), our scan over M_0 is performed in the range from 10^3 GeV to 10^6 GeV. The results show that for each value of M_0 there exist two values of μ that accommodate a successful leptogenesis, and the ratio of μ to M_0 is about 10^{-10} or 10^{-14} (10^{-9} or 10^{-21}) in the NO (IO) cases. For the purpose of illustration, by taking $M_0 = 10^3$ GeV as a benchmark value, in Figure 4 we have shown the evolutions of η_N and η_B as functions of z . These results are obtained by taking the initial conditions to be $\eta_N^{\text{ini}} = \eta_B^{\text{ini}} = 0$. The results show that, for the benchmark value $M_0 = 10^3$ GeV, the observed value of η_B can be successfully reproduced for $\mu \simeq 10^{-8.4}$ GeV ($10^{-5.9}$ GeV) in the NO (IO) case.

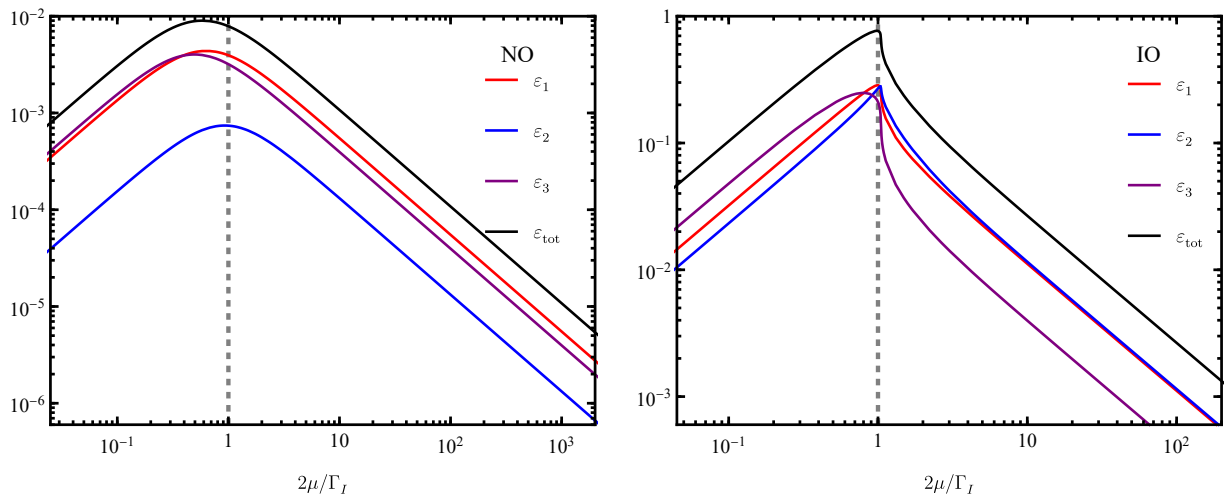


Figure 1: For the modular A_4 symmetry model given in section 3, in the scenario that the mass splittings among the three right-handed neutrinos are realized by modifying M_R into the form as shown in Eq. (7), CP asymmetries in the decays of N_I as functions of the ratio $2\mu/\Gamma_I$ in the NO (left panel) and IO (right panel) cases. Here $\varepsilon_{\text{tot}} = \varepsilon_1 + \varepsilon_2 + \varepsilon_3$ has been defined.

Then, we consider the scenario that the mass splittings among the three right-handed neutrinos are

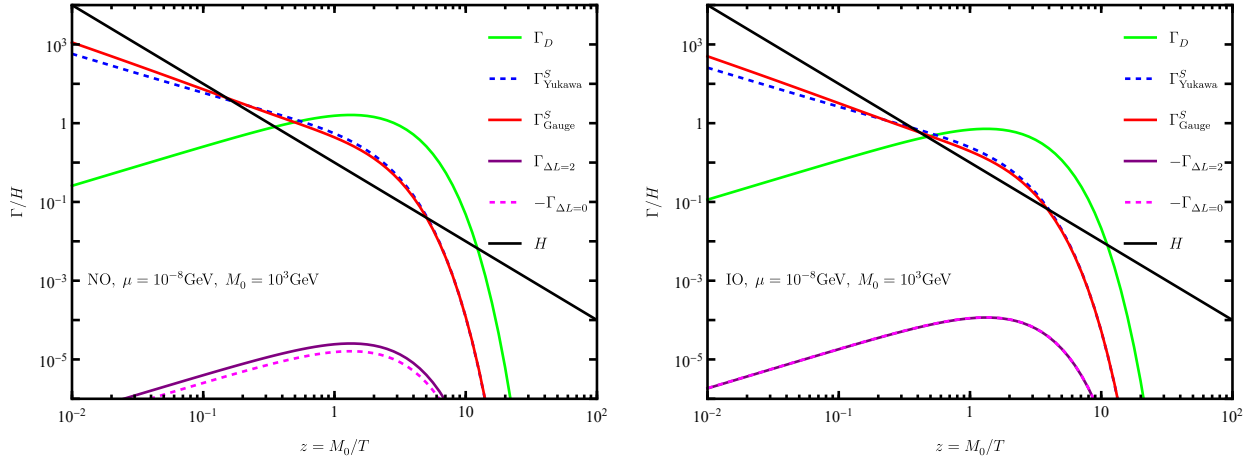


Figure 2: For the modular A_4 symmetry model given in section 3, in the scenario that the mass splittings among the three right-handed neutrinos are realized by modifying M_R into the form as shown in Eq. (7), the various collision terms in the Boltzmann equations as functions of $z = M_0/T$ in the NO (left panel) and IO (right panel) cases. These results are obtained by taking $M_0 = 10^3$ GeV and $\mu = 10^{-8}$ GeV as benchmark values.

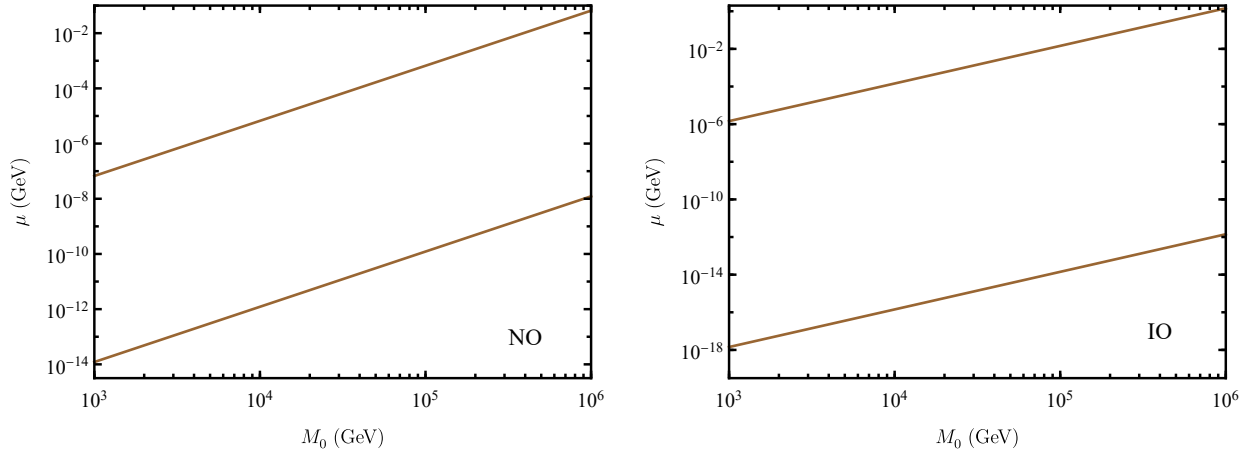


Figure 3: For the modular A_4 symmetry model given in section 3, in the scenario that the mass splittings among the three right-handed neutrinos are realized by modifying M_R into the form as shown in Eq. (7), the values of μ that accommodate a successful leptogenesis as functions of M_0 in the NO (left panel) and IO (right panel) cases.

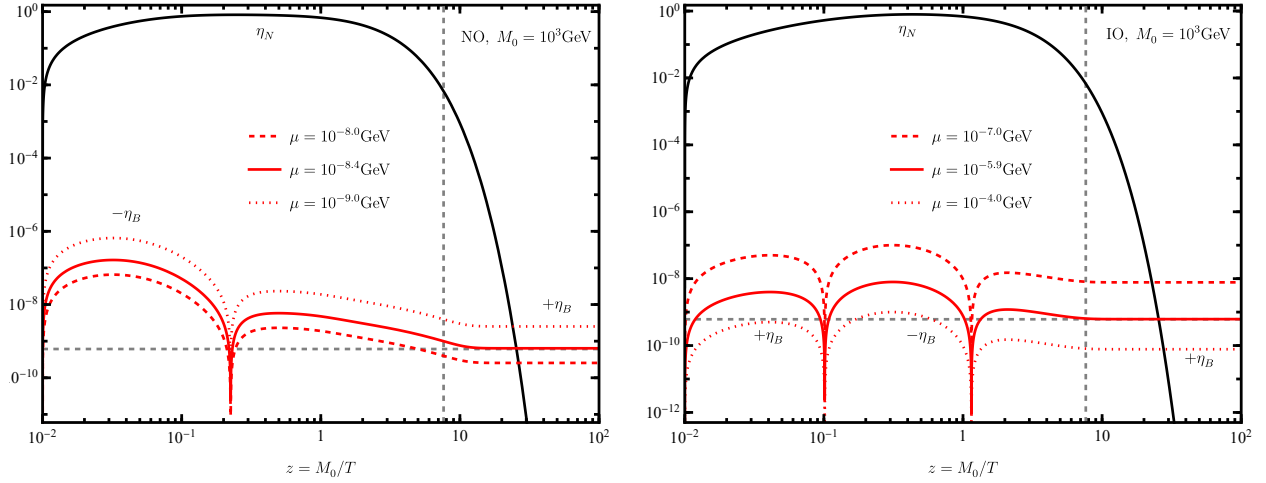


Figure 4: For the modular A_4 symmetry model given in section 3, in the scenario that the mass splittings among the three right-handed neutrinos are realized by modifying M_R into the form as shown in Eq. (7), the evolutions of η_N and η_B as functions of z for the benchmark value $M_0 = 10^3$ GeV and some benchmark values of μ in the NO (left panel) and IO (right panel) cases. Here the horizontal grey dashed line shows the observed value of η_B (same as below) and the vertical dotted line represents the decoupling temperature $T_* \simeq 131.7$ GeV of sphalerons [21].

generated from the RGE effects. In this regard, Figure 5 has shown the RGE-induced mass splittings of the three right-handed neutrinos. In obtaining these results, we have fixed the flavor-symmetry scale Λ_{FS} at the grand unification (GUT) scale 10^{16} GeV. The results show that the ratios $\Delta M_{IJ}/M_0$ (for $\Delta M_{IJ} \equiv M_I - M_J$) are linearly proportional to M_0 . This is because $\Delta M_{IJ}/M_0$ are proportional to YY^\dagger [see Eq. (23)], which in turn is proportional to M_0 because of the seesaw relationship [see Eq. (3)]. Figure 6 further shows the CP asymmetries in the decays of N_I as functions of M_0 . In the NO case, for $M_0 < 10^{11}$ GeV, the CP asymmetries are small and nearly independent of M_0 . But for $M_0 > 10^{11}$ GeV, ε_3 increases rapidly with M_0 , while ε_1 and ε_2 also do so after a sign reversal from being positive to negative. In the IO case, the CP asymmetries keep positive and change very slowly as M_0 increases. Finally, Figure 7 has shown the generated η_B as functions of M_0 . As one can see, the observed value of η_B can be successfully reproduced for $M_0 \simeq 6 \times 10^{12}$ GeV (4×10^{12} GeV or 6×10^{12} GeV) in the NO (IO) case. These results can be understood with the help of the results in Figure 6.

4 Study for modular S_4 symmetry model

In Ref. [22], the authors have presented a comprehensive analysis of neutrino masses and mixing in theories with modular S_4 symmetry. In the case that the three right-handed neutrinos have a weight $k_{Nc} = 0$ and constitute the $\mathbf{3}$ or $\mathbf{3}'$ representation of S_4 , the right-handed neutrino mass matrix will take a same form as in Eq. (5). When the three left-handed lepton doublets have a weight $k_L = 2$ and constitute the same three-dimensional representation of S_4 as the three right-handed neutrinos, the Dirac

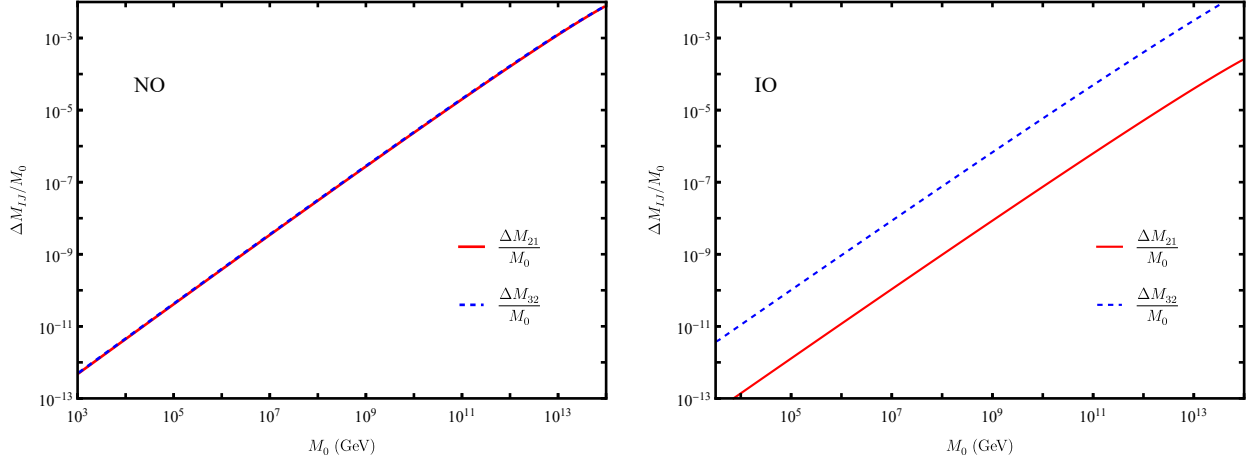


Figure 5: For the modular A_4 symmetry model given in section 3, in the scenario that the mass splittings among the three right-handed neutrinos are generated from the RGE effects, $\Delta M_{IJ}/M_0$ (for $\Delta M_{IJ} \equiv M_I - M_J$) as functions of M_0 in the NO (left panel) and IO (right panel) cases.

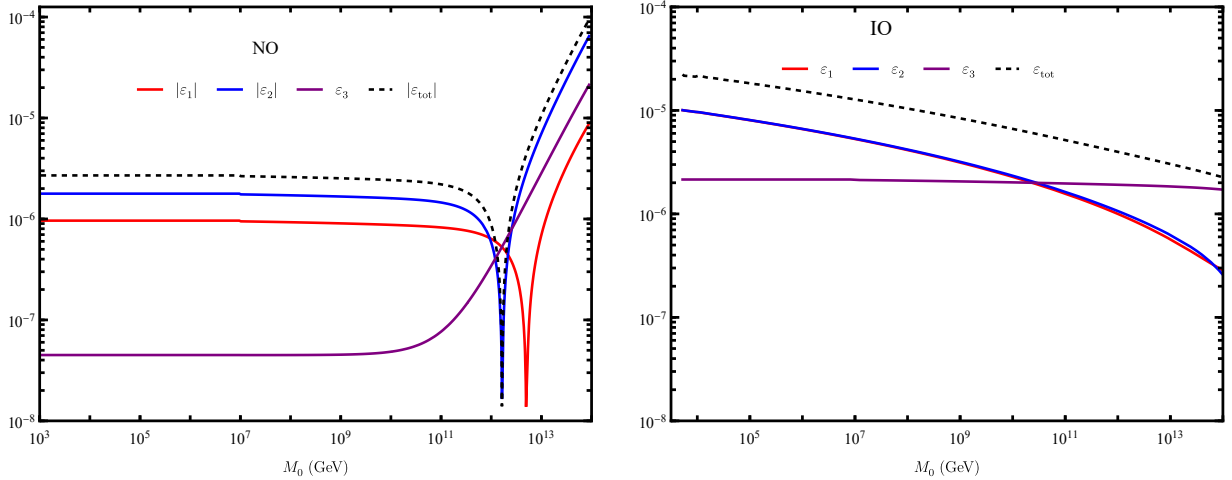


Figure 6: For the modular A_4 symmetry model given in section 3, in the scenario that the mass splittings among the three right-handed neutrinos are generated from the RGE effects, the CP asymmetries in the decays of N_I as functions of M_0 in the NO (left panel) and IO (right panel) cases.

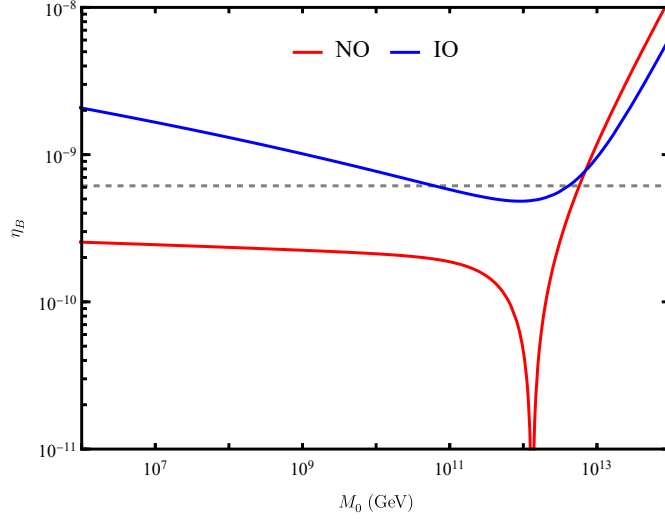


Figure 7: For the modular A_4 symmetry model given in section 3, in the scenario that the mass splittings among the three right-handed neutrinos are generated from the RGE effects, the generated η_B as functions of M_0 in the NO (in the red color) and IO (in the blue color) cases.

neutrino mass matrix will take a form as

$$M_D = gv_u \left[\begin{pmatrix} 0 & Y_1 & Y_2 \\ Y_1 & Y_2 & 0 \\ Y_2 & 0 & Y_1 \end{pmatrix} + \frac{g'}{g} \begin{pmatrix} 0 & Y_5 & -Y_4 \\ -Y_5 & 0 & Y_3 \\ Y_4 & -Y_3 & 0 \end{pmatrix} \right]. \quad (31)$$

If the three left-handed lepton doublets constitute a three-dimensional representation of S_4 different from the three right-handed neutrinos, then the Dirac neutrino mass matrix will take a form as

$$M_D = gv_u \left[\begin{pmatrix} 0 & -Y_1 & Y_2 \\ -Y_1 & Y_2 & 0 \\ Y_2 & 0 & -Y_1 \end{pmatrix} + \frac{g'}{g} \begin{pmatrix} 2Y_3 & -Y_5 & -Y_4 \\ -Y_5 & 2Y_4 & -Y_3 \\ -Y_4 & -Y_3 & 2Y_5 \end{pmatrix} \right]. \quad (32)$$

On the other hand, for the minimal (in terms of weights) possibility, the charged-lepton mass matrix takes a form as

$$M_l = v_d \begin{pmatrix} \alpha Y_3 & \alpha Y_5 & \alpha Y_4 \\ \beta (Y_1 Y_4 - Y_2 Y_5) & \beta (Y_1 Y_3 - Y_2 Y_4) & \beta (Y_1 Y_5 - Y_2 Y_3) \\ \gamma (Y_1 Y_4 + Y_2 Y_5) & \gamma (Y_1 Y_3 + Y_2 Y_4) & \gamma (Y_1 Y_5 + Y_2 Y_3) \end{pmatrix}. \quad (33)$$

In the above three equations, g , g' , α , β and γ are simply dimensionless parameters, while Y_i are modular forms of weight 2 and level 4 whose explicit expressions have been formulated in Ref. [23].

One can see that this model also contains 8 real parameters in total: αv_d , β/α , γ/α , $g^2 v_u^2/M_0$, $|g'/g|$, $\arg(g'/g)$, $\text{Re}(\tau)$ and $\text{Im}(\tau)$. The numerical calculation shows that this model can be consistent with the neutrino oscillation experimental results. For M_D in Eq. (31), the model can be consistent with the neutrino oscillation experimental results only in the NO case, and the numerical search finds two pairs of distinct local minima of $\Delta\chi^2$ corresponding to two pairs of distinct values of τ . The two minima in each pair lead to opposite values of the Dirac and Majorana phases, but the same values of all other

observables. The cases belonging to the first pair are denoted as Case A, while those belonging to the second pair are denoted as Case B. For these two cases, the resulting predictions for the best-fit values and the allowed ranges of the input parameters and observables are collected in Table 3 [22]. For M_D in Eq. (32), the model can be consistent with the neutrino oscillation experimental results in both the NO and IO cases. In the IO case, the numerical search finds two pairs of distinct local minima of $\Delta\chi^2$ corresponding to two pairs of distinct values of τ , and the cases belonging to these two pairs are respectively denoted as Case C and Case D. In the NO case, the numerical search only finds one pair of local minima of $\Delta\chi^2$ corresponding to one pair of distinct values of τ , and the cases belonging to this pair are denoted as Case E. For these three cases, the resulting predictions for the best-fit values and the allowed ranges of the input parameters and observables are collected in Table 4 [22].

	Case A (NO)		Case B (NO)	
	Best-fit	Allowed regions	Best-fit	Allowed regions
$\text{Re}(\tau)$	± 0.1045	$\pm(0.09378 - 0.1128)$	∓ 0.109	$\mp(0.103 - 0.1197)$
$\text{Im}(\tau)$	1.01	1.004 – 1.018	1.005	0.9988 – 1.008
β/α	9.465	7.693 – 12.39	0.03306	0.02529 – 0.04074
γ/α	0.002205	0.001941 – 0.002472	0.0001307	0.0000982 – 0.0001663
$\text{Re}(g'/g)$	0.233	–0.02544 – 0.4417	0.4097	0.3241 – 0.5989
$\text{Im}(g'/g)$	± 0.4924	$\pm(-0.6046 - 0.5751)$	∓ 0.5745	$\mp(0.5436 - 0.5944)$
αv_d [MeV]	53.19	—	893.2	—
$g^2 v_u^2/M_0$ [eV]	0.00467	—	0.004014	—
m_e/m_μ	0.004802	0.00422 – 0.005383	0.004802	0.004211 – 0.005384
m_μ/m_τ	0.0565	0.04317 – 0.06961	0.05649	0.04318 – 0.06962
$\sin^2 \theta_{12}$	0.305	0.2656 – 0.3449	0.305	0.2662 – 0.3455
$\sin^2 \theta_{13}$	0.02125	0.01912 – 0.02383	0.02125	0.01914 – 0.02383
$\sin^2 \theta_{23}$	0.551	0.4838 – 0.5999	0.551	0.4322 – 0.601
m_1 [eV]	0.01746	0.01185 – 0.02143	0.02074	0.01918 – 0.02428
m_2 [eV]	0.01945	0.01473 – 0.02307	0.02244	0.02101 – 0.02574
m_3 [eV]	0.05288	0.05075 – 0.05452	0.05406	0.05314 – 0.05577
δ/π	± 1.314	$\pm(1.249 - 1.961)$	± 1.919	$\pm(1.882 - 1.977)$
α_{21}/π	± 0.302	$\pm(0.2748 - 0.3708)$	± 1.704	$\pm(1.681 - 1.722)$
α_{31}/π	± 0.8716	$\pm(0.7973 - 1.635)$	± 1.539	$\pm(1.484 - 1.618)$
$N\sigma \equiv \sqrt{\Delta\chi^2}$	0.02005	—	0.02435	—

Table 3: For the model given in section 4 with M_D in Eq. (31), in the phenomenologically viable NO case, the predictions for the best-fit values and the allowed ranges of the input parameters and observables in Case A and Case B. These results are taken from Tables 5a-5b in Ref. [22].

	Case C (IO)		Case D (IO)		Case E (NO)	
	Best-fit	Allowed regions	Best-fit	Allowed regions	Best-fit	Allowed regions
$\text{Re}(\tau)$	∓ 0.1435	$\mp(0.1222 - 0.168)$	± 0.179	$\pm(0.1589 - 0.199)$	∓ 0.4996	$\mp(0.48 - 0.5084)$
$\text{Im}(\tau)$	1.523	1.088 – 1.594	1.397	1.236 – 1.529	1.309	1.246 – 1.385
β/α	17.82	9.32 – 23.66	15.35	10.79 – 21.09	0.000243	0.0002004 – 0.0002864
γ/α	0.003243	0.00227 – 0.003733	0.002924	0.002443 – 0.003459	0.03335	0.02799 – 0.03926
$\text{Re}(g'/g)$	-0.8714	-(0.7956 – 1.148)	-1.32	-(1.131 – 1.447)	-0.06454	-(0.01697 – 0.1215)
$\text{Im}(g'/g)$	∓ 2.094	$\mp(1.409 - 2.182)$	± 1.733	$\pm(1.306 - 2.017)$	∓ 0.569	$\mp(0.4572 - 0.6564)$
αv_d [MeV]	71.26	—	68.42	—	1125	—
$g^2 v_u^2/M_0$ [eV]	0.004087	—	0.00447	—	0.0087	—
m_e/m_μ	0.004797	0.004215 – 0.005378	0.004786	0.004221 – 0.005386	0.004797	0.004393 – 0.005197
m_μ/m_τ	0.05655	0.04348 – 0.0698	0.0554	0.04343 – 0.06968	0.05626	0.04741 – 0.0654
$\sin^2 \theta_{12}$	0.303	0.2657 – 0.3436	0.3031	0.2657 – 0.3436	0.311	0.2895 – 0.3375
$\sin^2 \theta_{13}$	0.02175	0.01957 – 0.0242	0.02184	0.01954 – 0.0242	0.02185	0.02041 – 0.02351
$\sin^2 \theta_{23}$	0.5571	0.4551 – 0.6026	0.5577	0.5482 – 0.6013	0.4469	0.43 – 0.4614
m_1 [eV]	0.0513	0.04882 – 0.05207	0.05122	0.05023 – 0.05212	0.01774	0.01703 – 0.01837
m_2 [eV]	0.05201	0.04958 – 0.05274	0.05193	0.05098 – 0.05279	0.0197	0.01906 – 0.02025
m_3 [eV]	0.01512	0.00316 – 0.0163	0.01495	0.01223 – 0.01649	0.05299	0.05251 – 0.05346
δ/π	± 1.098	$\pm(0.98 - 1.289)$	± 1.384	$\pm(1.271 - 1.437)$	± 1.601	$\pm(1.287 - 1.828)$
α_{21}/π	± 1.241	$\pm(1.113 - 1.758)$	± 1.343	$\pm(1.171 - 1.479)$	± 1.093	$\pm(0.8593 - 1.178)$
α_{31}/π	± 0.2487	$\pm(0.069 - 0.346)$	± 0.806	$\pm(0.448 - 1.149)$	± 0.7363	$\pm(0.3334 - 0.9643)$
$N\sigma \equiv \sqrt{\Delta\chi^2}$	0.0357	—	0.3811	—	2.147	—

Table 4: For the model given in section 4 with M_D in Eq. (32), in their respective phenomenologically viable neutrino mass ordering cases, the predictions for the best-fit values and the allowed ranges of the input parameters and observables in Case C, Case D and Case E. These results are taken from Tables 5c-5e in Ref. [22].

Now, in a similar way as in section 3, we study the consequences of these five cases for tri-resonant leptogenesis in the scenarios that the mass splittings among the three right-handed neutrinos are realized by modifying M_R into the form as shown in Eq. (7) and generated from the RGE effects, respectively. For the former scenario, the left panel of Figure 8 has shown the total CP asymmetries ε_{tot} in the decays of N_I as functions of $2\mu/\Gamma_{\text{tot}}$. We see that the results in these five cases are very similar to one another, and the CP asymmetries can take their maximally allowed values around $2\mu/\Gamma_{\text{tot}} \sim 1$. This will be helpful for us to reproduce the observed value of η_B . The right panel of Figure 8 has shown the values of μ that accommodate a successful leptogenesis as functions of M_0 . The results for the five cases are very similar to one another, and the ratios of μ to M_0 are around 10^{-9} or 10^{-18} at $M_0 = 10^3$ GeV. For the latter scenario, the left panel of Figure 9 has shown the total CP asymmetries ε_{tot} in the decays of N_I as functions of M_0 , while the right panel of Figure 9 has shown the generated η_B as functions of M_0 . These results have also been obtained by taking $\Lambda_{\text{FS}} = 10^{16}$ GeV. The results show that only for Case E and

$M_0 \sim 10^{12}$ GeV can the observed value of η_B be successfully reproduced, while the the magnitudes of η_B are always larger than its observed value in the other four cases. It is interesting to recall that Case E holds in the NO case which is slightly preferred by the current experimental results compared to the IO case [2, 3].

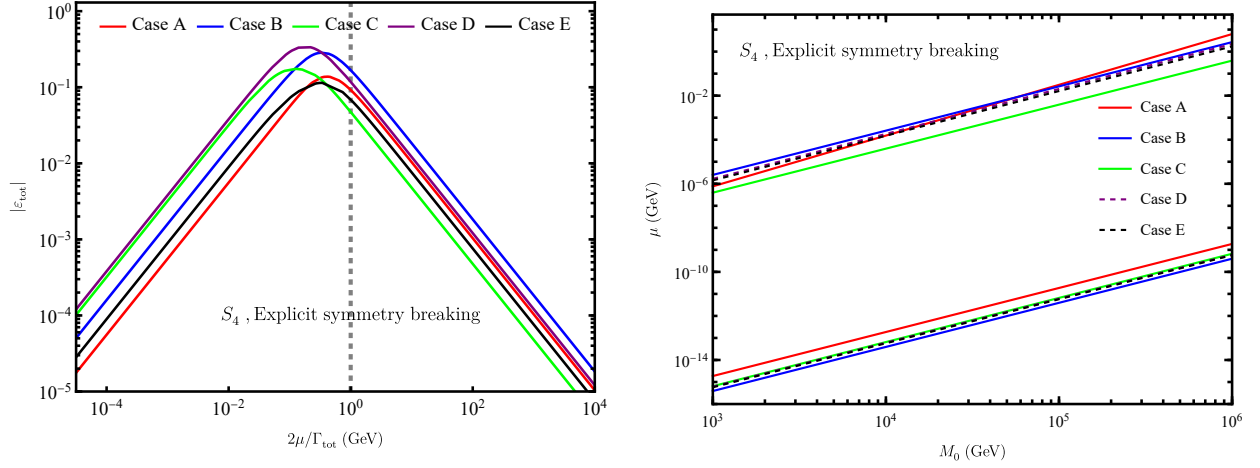


Figure 8: For the modular S_4 symmetry model given in section 4, in the scenario that the mass splittings among the three right-handed neutrinos are realized by modifying M_R into the form as shown in Eq. (7), the total CP asymmetries ε_{tot} in the decays of N_I as functions of $2\mu/\Gamma_{\text{tot}}$ (left panel), and the values of μ that accommodate a successful leptogenesis as functions of M_0 (right panel).

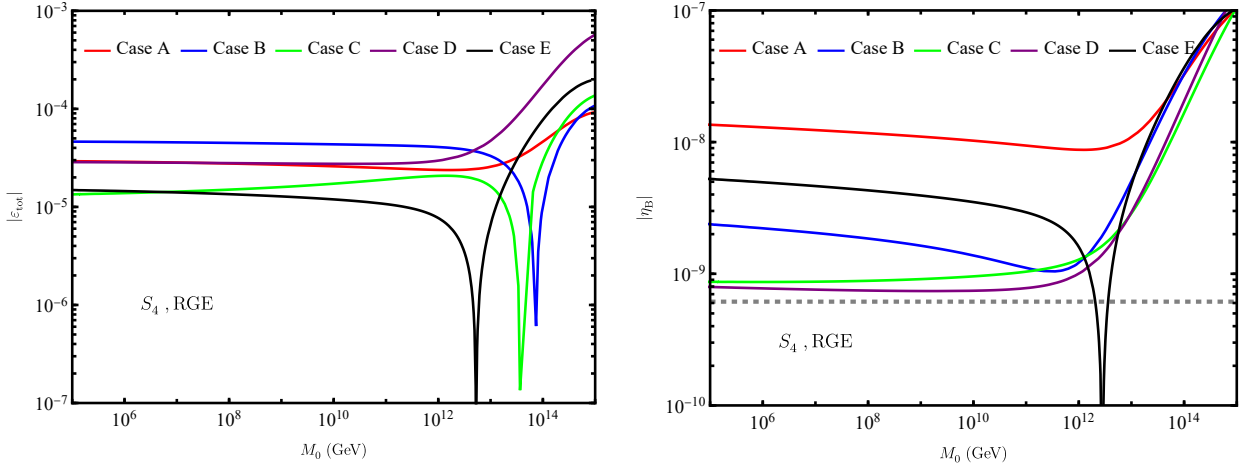


Figure 9: For the modular S_4 symmetry model given in section 4, in the scenario that the mass splittings among the three right-handed neutrinos are generated from the RGE effects, the total CP asymmetries ε_{tot} in the decays of N_I as functions of M_0 (left panel), and the generated η_B as functions of M_0 (right panel).

5 Study for modular A_5 symmetry model

In Ref. [24], the authors have presented a comprehensive analysis of neutrino masses and mixing in theories with modular A_5 symmetry. A_5 is the symmetry group of even permutations of 5 objects, and it has one singlet representation $\mathbf{1}$, two three-dimensional representations $\mathbf{3}$ and $\mathbf{3}'$, one four-dimensional representation $\mathbf{4}$ and one five-dimensional representation $\mathbf{5}$. In that paper, the authors have constructed modular-invariant models in which all leptons are collected into $\mathbf{3}$ or $\mathbf{3}'$ multiplets of A_5 , containing the three generations of each type of field. The neutrino sector has been taken to be minimal and it only depends on the modulus τ and an overall scale. But modular forms do not appear in the charged-lepton sector, which instead contains two extra flavons. In the case that the three right-handed neutrinos have a weight $k_{Nc} = 0$ and constitute the $\mathbf{3}$ representation of A_5 , the right-handed neutrino mass matrix will take a same form as in Eq. (5). When the three left-handed lepton doublets have a weight $k_L = -2$ and constitute $\mathbf{3}'$ representation of A_5 , the Dirac neutrino mass matrix will take a form as

$$M_D = y_0 v_u \begin{pmatrix} \sqrt{3}Y_1 & Y_4 & Y_3 \\ Y_5 & -\sqrt{2}Y_3 & -\sqrt{2}Y_2 \\ Y_2 & -\sqrt{2}Y_5 & -\sqrt{2}Y_4 \end{pmatrix}. \quad (34)$$

On the other hand, for the minimal (in terms of weights) possibility, the charged-lepton mass matrix takes a form as

$$M_l = v_d \begin{pmatrix} \alpha + 4\gamma(1 - \varphi_2\varphi_3) & (\beta + 6\gamma)\varphi_3 & (-\beta + 6\gamma)\varphi_2 \\ (-\beta + 6\gamma)\varphi_3 & 6\gamma\varphi_3^2 & \alpha + \beta - 2\gamma(1 - \varphi_2\varphi_3) \\ (\beta + 6\gamma)\varphi_2 & \alpha - \beta - 2\gamma(1 - \varphi_2\varphi_3) & 6\gamma\varphi_2^2 \end{pmatrix}. \quad (35)$$

In the above two equations, y_0 , α , β and γ are simply dimensionless parameters, φ_2 and φ_3 are the VEVs of relevant flavon fields and will be treated as free parameters, while Y_i are modular forms of weight 2 and level 5 whose explicit expressions have been formulated in Ref. [25].

Similar to the models in sections 3 and 4, in the present model the charged-lepton masses are essentially controlled by αv_d , β/α and γ/α , while the neutrino masses and mixing angles are mainly governed by $y_0^2 v_u^2/M_0$, τ , φ_2 and φ_3 . The number of parameters is further reduced by enforcing the CP conservation which restricts all the Yukawa couplings together with φ_2 and φ_3 to be real (with the VEV of τ serving as the only source of CP violation). The numerical calculation shows that this model can be consistent with the neutrino oscillation experimental only in the NO case and it further predicts $m_1 = 0$. The resulting predictions for the best-fit values of the input parameters and observables are collected in Table 5.

For this model, in a similar way as in sections 3 and 4, we study the consequences of it for tri-resonant leptogenesis in the scenarios that the mass splittings among the three right-handed neutrinos are realized by modifying M_R into the form as shown in Eq. (7) and generated from the RGE effects, respectively. For the former scenario, the left panel of Figure 10 has shown the values of μ that accommodate a successful leptogenesis as functions of M_0 . The results show that the ratio of μ to M_0 is around 10^{-8} or 10^{-10} at $M_0 = 10^3$ GeV. For the latter scenario, the right panel of Figure 10 has shown the generated η_B as functions of M_0 . These results have also been obtained by taking $\Lambda_{FS} = 10^{16}$ GeV. The results show that the observed value of η_B can not be successfully reproduced.

$\text{Re}(\tau)$	$\text{Im}(\tau)$	φ_2	φ_3	$\alpha \cos \beta \cdot 10^3$	β/α	γ/α	$y_0^2 \sin^2 \beta / M_0$ (eV $^{-1}$)
-0.3615	0.2412	0.04759	0.3731	3.368	1.310	-0.2413	0.0001639

$m_1 \cdot 10^2$ eV $^{-1}$	$m_2 \cdot 10^2$ eV $^{-1}$	$m_3 \cdot 10^2$ eV $^{-1}$	$\sin^2 \theta_{12}$	$\sin^2 \theta_{13}$	$\sin^2 \theta_{23}$	δ/π	$(\alpha_{21}-\alpha_{31})/\pi$	χ_{\min}^2
0	0.860	5.02	0.292	0.0228	0.449	1.63	1.68	11.1

Table 5: For the model given in section 5, in the phenomenologically viable NO case, the predictions for the best-fit values of the input parameters and observables. These results are taken from Tables 8 in Ref. [24].

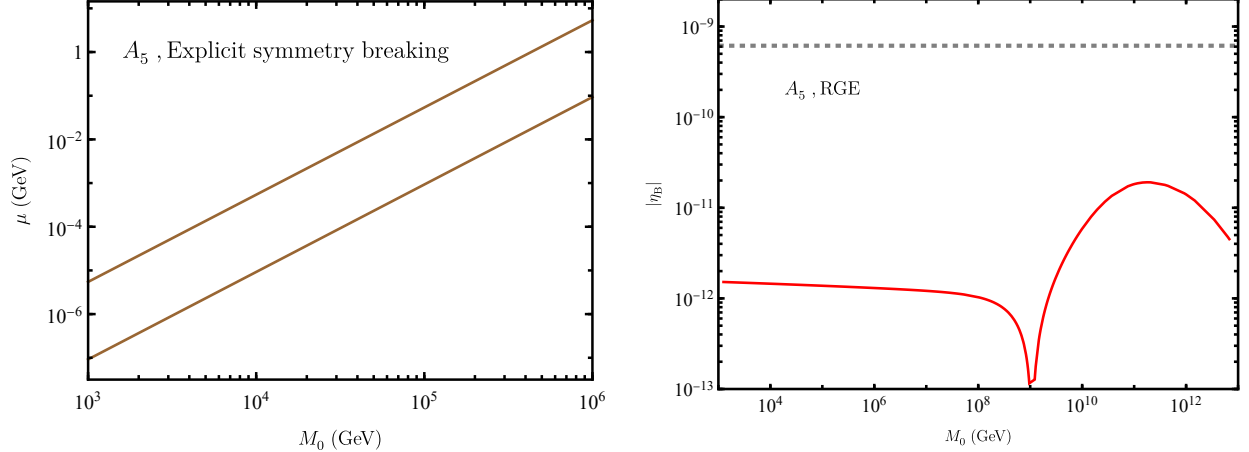


Figure 10: For the modular A_5 symmetry model given in section 5, in the scenario that the mass splittings among the three right-handed neutrinos are realized by modifying M_R into the form as shown in Eq. (7), the values of μ that accommodate a successful leptogenesis as functions of M_0 (left panel). In the scenario that the mass splittings among the three right-handed neutrinos are generated from the RGE effects, the generated η_B as functions of M_0 (right panel).

6 Summary

As we know, due to the peculiarity of the observed neutrino mixing pattern, there have been intensive model-building studies on neutrino-related physics with the employment of certain discrete non-Abelian symmetries. However, a shortcoming of the conventional flavor-symmetry models is that many flavon fields need to be introduced in order to achieve a desired breaking pattern of the flavor symmetry, and the scalar potential of these flavon fields needs a complicated symmetric shaping. In recent years, the idea of modular invariance which provides substantial simplifications to these problems has been proposed and become increasingly popular.

However, for some typical modular symmetry neutrino models, the right-handed neutrino mass matrix takes a form as shown in Eq. (5) which gives three degenerate right-handed neutrino masses and consequently prohibits the leptogenesis to work. But this kind of models can serve as a unique basis for realizations of the tri-resonant leptogenesis scenario: if the right-handed neutrino masses receive certain corrections so that their degeneracy is lifted to an appropriate extent, then the tri-resonant leptogenesis

scenario will be naturally realized. In this paper, we have considered two minimal ways to generate the desired small mass splittings among the three right-handed neutrinos: one way is to modify M_R to a form as shown in Eq. (7), while another way is to consider the renormalization-group corrections for the right-handed neutrino masses.

To be specific, we have considered modular A_4 , S_4 and A_5 symmetry models that have a right-handed neutrino mass matrix as shown in Eq. (5). For these models, in the scenario that the mass splittings among the three right-handed neutrinos are realized by modifying M_R into the form as shown in Eq. (7), the observed value of η_B can always be successfully reproduced for appropriate values of μ . These results can be easily understood from the fact that given that μ is a free parameter, the resonance conditions which enhance the CP asymmetries to their maximally allowed values can always be fulfilled (this is of course helpful for us to reproduce the observed value of η_B).

However, for the scenario that the mass splittings among the three right-handed neutrinos are generated from the RGE effects, the results will be highly restrictive. Having fixed the flavor-symmetry scale to be at the GUT scale, we reach the following conclusions for the considered representative models:

- For the modular A_4 symmetry model given in section 3, the observed value of η_B can be successfully reproduced for $M_0 \simeq 6 \times 10^{12}$ GeV (4×10^{12} GeV or 6×10^{12} GeV) in the NO (IO) case.
- For the modular S_4 symmetry model given in section 4, among the five cases, only for Case E (which holds in the NO case) and $M_0 \sim 10^{12}$ GeV can the observed value of η_B be successfully reproduced.
- For the modular A_5 symmetry model given in section 5, the observed value of η_B can not be successfully reproduced.

Acknowledgments

This work is supported in part by the National Natural Science Foundation of China under grant Nos. 11605081, 12142507 and 12147214, the Natural Science Foundation of the Liaoning Scientific Committee under grant NO. 2022-MS-314, and the Ph. D. Research Start-up Fund of Anyang Institute of Technology (no. BSJ2021048).

References

- [1] Z. Z. Xing, Phys. Rep. **854**, 1 (2020).
- [2] I. Esteban, M. C. Gonzalez-Garcia, M. Maltoni, T. Schwetz and A. Zhou, JHEP **09**, 178 (2020); NuFIT 5.2 (2022), www.nu-fit.org.
- [3] F. Capozzi, E. D. Valentino, E. Lisi, A. Marrone, A. Melchiorri and A. Palazzo, Phys. Rev. D **104**, 083031 (2021); P. F. de Salas, D. V. Forero, S. Gariazzo, P. Martinez-Mirave, O. Mena, M. Tortola and J. W. F. Valle, JHEP **02**, 071 (2021).

- [4] For some reviews, see W. Rodejohann, *Int. J. Mod. Phys. E* **20**, 1833 (2011); S. M. Bilenky and C. Giunti, *Int. J. Mod. Phys. A* **30**, 0001 (2015); S. Dell’Oro, S. Marcocci, M. Viel and F. Vissani, *Adv. High Energy Phys.* **2016**, 2162659 (2016); J. D. Vergados, H. Ejiri and F. Simkovic, *Int. J. Mod. Phys. E* **25**, 1630007 (2016); M. J. Dolinski, A. W. P. Poon and W. Rodejohann, *Ann. Rev. Nucl. Part. Sci.* **69**, 219 (2019).
- [5] P. F. Harrison, D. H. Perkins and W. G. Scott, *Phys. Lett. B* **530**, 167 (2002); Z. Z. Xing, *Phys. Lett. B* **533**, 85 (2002).
- [6] S. F. King and C. Luhn, *Rept. Prog. Phys.* **76**, 056201 (2013); F. Feruglio and A. Romanino, *Rev. Mod. Phys.* **93**, 015007 (2021); G. J. Ding and J. W.F. Valle, arXiv:2402.16963.
- [7] F. Feruglio, arXiv:1706.08749.
- [8] For a review with extensive references, see G. J. Ding, and S. F. King, arXiv:2311.09282.
- [9] P. Minkowski, *Phys. Lett. B* **67**, 421 (1977); M. Gell-Mann, P. Ramond and R. Slansky, in *Supergravity*, edited by P. van Nieuwenhuizen and D. Freedman, (North-Holland, 1979), p. 315; T. Yanagida, in *Proceedings of the Workshop on the Unified Theory and the Baryon Number in the Universe*, edited by O. Sawada and A. Sugamoto (KEK Report No. 79-18, Tsukuba, 1979), p. 95; R. N. Mohapatra and G. Senjanovic, *Phys. Rev. Lett.* **44**, 912 (1980); J. Schechter and J. W. F. Valle, *Phys. Rev. D* **22**, 2227 (1980).
- [10] M. Fukugita and T. Yanagida, *Phys. Lett. B* **174**, 45 (1986).
- [11] For some reviews, see W. Buchmuller, R. D. Peccei and T. Yanagida, *Ann. Rev. Nucl. Part. Sci.* **55**, 311 (2005); W. Buchmuller, P. Di Bari and M. Plumacher, *Annals Phys.* **315**, 305 (2005); S. Davidson, E. Nardi and Y. Nir, *Phys. Rept.* **466**, 105 (2008).
- [12] P. A. R. Ade *et al.* (Planck Collaboration), *Astron. Astrophys. A* **16**, 571 (2014).
- [13] S. Davidson and A. Ibarra, *Phys. Lett. B* **535**, 25 (2002).
- [14] A. Pilaftsis, *Phys. Rev. D* **56**, 5431 (1997); A. Pilaftsis and T. E. J. Underwood, *Nucl. Phys. B* **692**, 303 (2004); P. Candia da Silva, D. Karamitros, T. McKelvey and A. Pilaftsis, *JHEP* **11**, 065 (2022).
- [15] A. M. Abdullahi *et al.*, *J. Phys. G* **50**, 020501 (2023).
- [16] X. Zhang and S. Zhou, *JHEP* **05**, 017 (2020).
- [17] R. Gonzalez Felipe, F. R. Joaquim and B. M. Nobre, *Phys. Rev. D* **70**, 085009 (2004); K. Turzynski, *Phys. Lett. B* **589**, 135 (2004); G. C. Branco, R. Gonzalez Felipe, F. R. Joaquim and B. M. Nobre, *Phys. Lett. B* **633**, 336 (2006); G. C. Branco, A. J. Buras, S. Jager, S. Uhlig and A. Weiler, *JHEP* **09**, 004 (2007).
- [18] A. Abada, S. Davidson, F. X. Josse-Michaux, M. Losada and A. Riotto, *JCAP* **0604**, 004 (2006); E. Nardi, Y. Nir, E. Roulet and J. Racker, *JHEP* **0601**, 164 (2006).

- [19] J. A. Casas, J. R. Espinosa, A. Ibarra and I. Navarro, Nucl. Phys. B **569**, 82 (2000); R. Gonzalez Felipe, F. R. Joaquim and B. M. Nobre, Phys. Rev. D **70**, 085009 (2004); G. C. Branco, A. J. Buras, S. Jager, S. Uhlig and A. Weiler, JHEP **09**, 004 (2007).
- [20] G. J. Ding, S. F. King and X. G. Liu, JHEP **09**, 074 (2019).
- [21] M. D'Onofrio, K. Rummukainen and A. Tranberg, Phys. Rev. Lett. **113**, 141602 (2014).
- [22] P. P. Novichkov, J. T. Penedo, S. T. Petcov and A. V. Titov, JHEP **04**, 005 (2019).
- [23] J. T. Penedo and S. T. Petcov, Nucl. Phys. B **939**, 292 (2019).
- [24] J. C. Criado, F. Feruglio and S. J. D. King, JHEP **02**, 001 (2020).
- [25] P. P. Novichkov, J. T. Penedo, S. T. Petcov and A. V. Titov, JHEP **04**, 174 (2019).